SLS Booster Radiation Environment

Anthony M. DeStefano
NASA, MSFC, EV44

April 26, 2021

Contents

List of Figures

List of Tables

1 Executive Summary

The purpose of the following update is to provide the Booster element with a low-altitude 50 km radiation environment. The SLS-SPEC-159 Cross-Program Design Specification for Natural Environments (DSNE) includes a 20 km and 200 km radiation environment, however the Booster element will only be achieving altitudes less than roughly 50 km. The updated 50 km radiation environment is derived following similar procedures as the generation of the 200 km radiation environment, as outlined in Section 3.2.13 of the DSNE. Specifically, tables for the linear energy transfer (LET), differential flux, and integral flux are given for the 50 km environment (see Tables 2, 3, and 4) and compared with DSNE Tables 3.2.13-1 – 3.2.13-3.

2 Reproducing DSNE 200 km Tables using CREME96

The 200 km LET (Linear Energy Transfer) and particle flux environments SLS-SPEC-159 Cross-Program Design Specification for Natural Environments (DSNE) were obtained using the Cosmic Ray Effects on Microelectrons 96 (CREME96[1]). In this section, DSNE Tables 3.2.13-1 – 3 are reproduced using the technical notes provided in the DSNE.

For the LET and flux, the GTRN routine is run using the following options:

- 1.C.a. & 1.C.b. 200 km circular orbit

- 1.C.c. 51.6 degrees orbit inclination

- 1.C.g. Effective L-shell range: $2.4 \leqslant L \leqslant 2.55$

- 2. Stormy magnetic weather conditions

2.1 Linear Energy Transfer (LET)

To compute the LET, the LETSPEC routine is used setting the following parameters:

- 2. and 3. $Z = 1$ to 92

- 4. particles > 0.1 MeV/nuc

- 5. Silicon target material

Integral LET due to solar particle events (SPEs) and galactic cosmic rays (GCRs) are both computed as shown in Figure 1. Agreement in both the SPE and GCR integral LET spectra show that the CREME96 inputs were interpreted correctly. The SPE LET integral flux includes a factor of $2\mathrm{x}$ on the CREME96 output to match what is in DSNE.

---

[1]https://creme.isde.vanderbilt.edu/

Figure 1: Output generated from CREME96 LETSPEC are plotted against DSNE Table 3.2.13-1 for SPEs and GCRs.

2.2 Differential Flux

The differential flux for both SPEs and GCRs are computed using the FLUX routine with the following options set:

SPE

- 1. and 2. $Z = 1$ to 92

- 2.a. CREME96

- 3.b. Worst Week

- 4. Inside Earth's Magnetosphere

GCR

- 1. and 2. $Z = 1$ to 92

- 2.a. CREME96

- 3.b. Solar Minimum (Cosmic-Ray Maximum)

- 4. Inside Earth's Magnetosphere

The differential flux output from CREME96 is plotted against Table 3.2.13-2 in Figure 2 and shows perfect agreement. Note that there is a factor of 2x on the SPEs from CREME96 to DSNE. According to the technical notes in DSNE, "The x2 multiplier of the 1989 event is needed to simulate a 'worst case' SPE exposure at the high 97% probability level..."
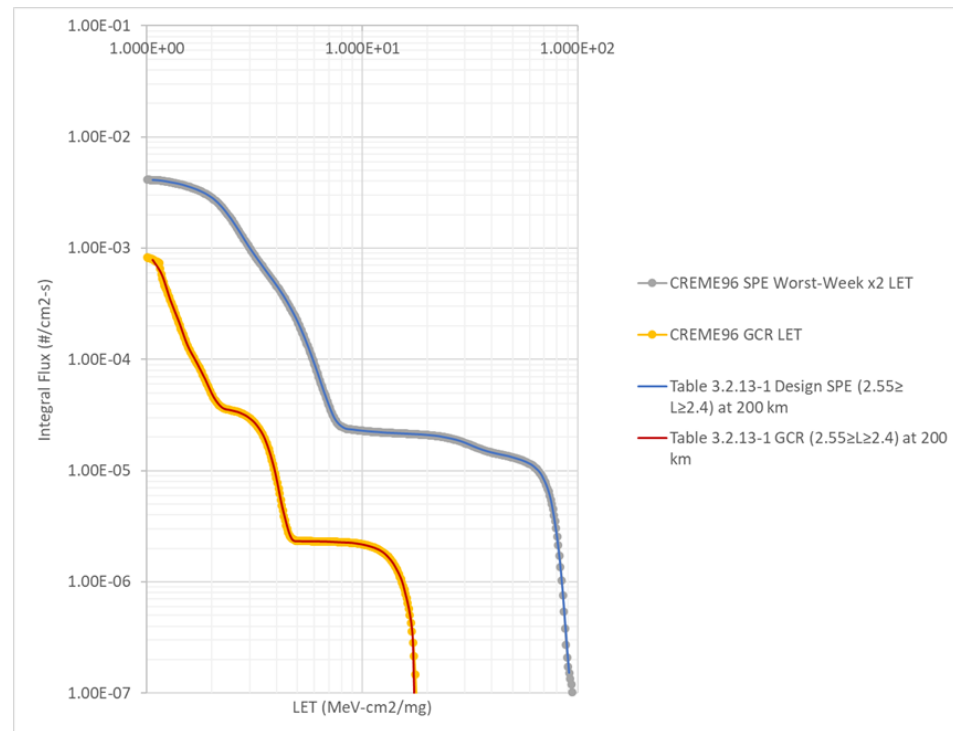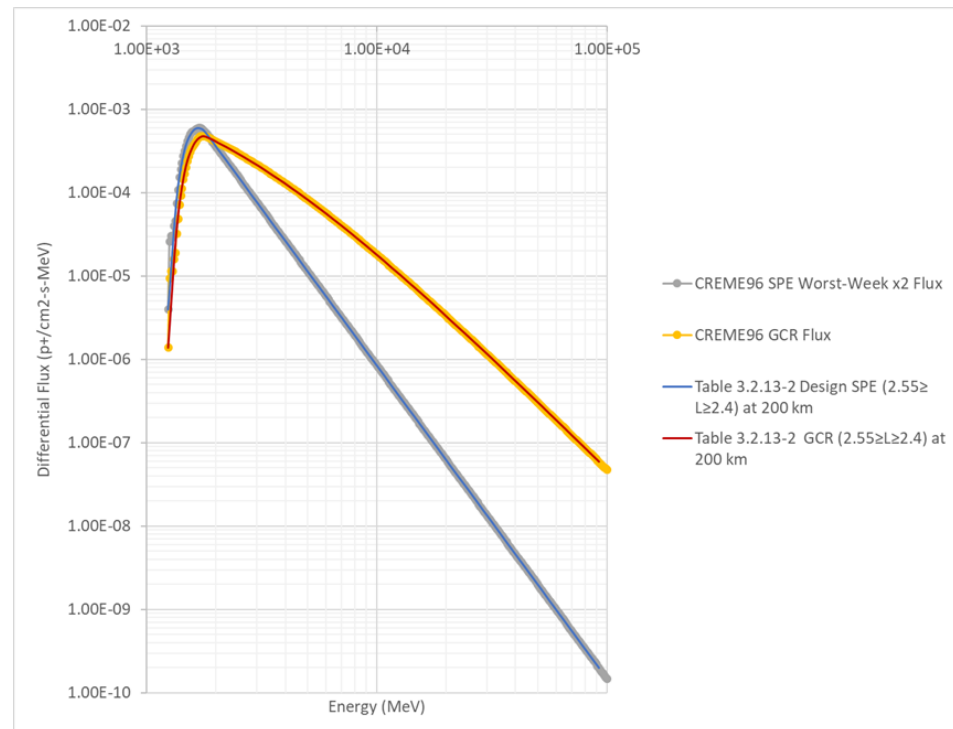
Figure 2: Output generated from CREME96 FLUX are plotted against DSNE Table 3.2.13-2 for SPEs and GCRs.

2.3 Integral Flux

The integral flux for both the SPEs and GRCs are derived from the differential flux output. Since the flux spectra have power-law-like features, the best way to approximate the differential flux is to interpolate using a power-law fit between data points (x_i, y_i), i.e.

$$y(x) = y_i \left(\frac{x}{x_i} \right)^{b_i}, \text{ for } x_i \leqslant x \leqslant x_{i+1}, \tag{1}$$

where

$$b_i = \frac{\log(y_{i+1}/y_i)}{\log(x_{i+1}/x_i)}. \tag{2}$$

The integral flux $(> x)$ can then be computed by integrating from some x to infinity

$$Y(> x) = \int_x^\infty dx' y(x'). \tag{3}$$

Inserting Equation (1) for $y(x)$, the integral flux becomes

$$Y(> x_n) = \sum_{i=n}^{N-1} \frac{y_i x_i}{b_i + 1} \left[\left(\frac{x_{i+1}}{x_i} \right)^{b_i + 1} - 1 \right]. \tag{4}$$

Applying Equation (4) to the differential fluxes shown in Section 2.2, the integral fluxes are derived and compared with DSNE Table 3.2.13-3 in Figure 3. The comparison again shows perfect agreement and also give merit to the power-law interpolation method outlined above.

Figure 3: Output generated from CREME96 FLUX and converted to integral fluxes using Equation (4) are plotted against DSNE Table 3.2.13-3 for SPEs and GCRs.

3   Updated 50 km Environment

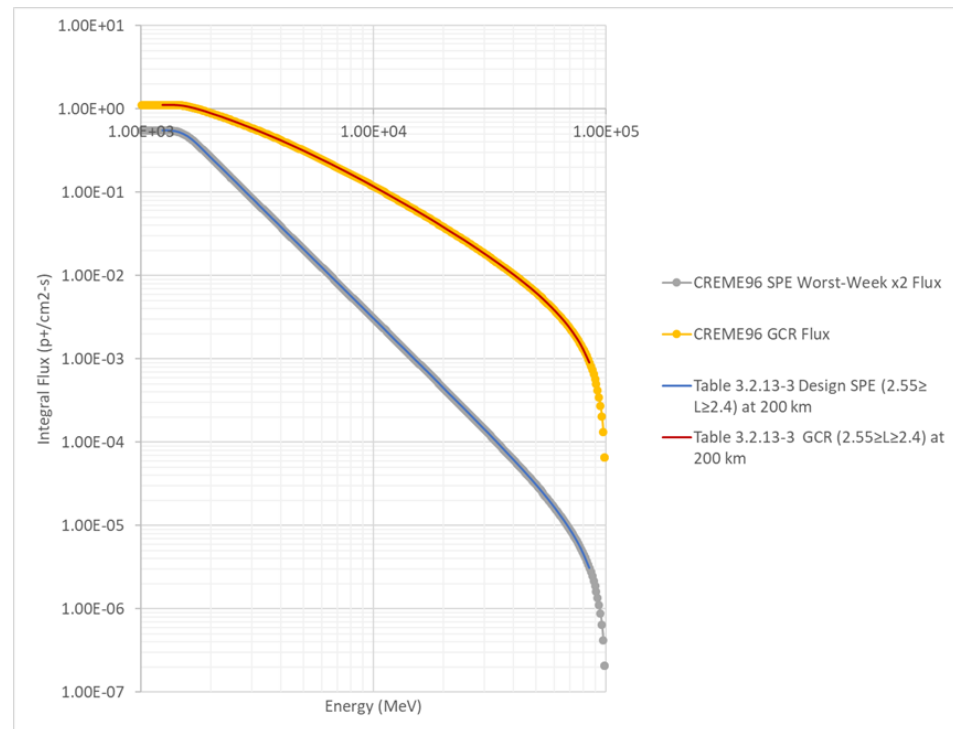In this section, the methods used to derive the DSNE tables for the 200 km environments will be used to compute the new 50 km environments. The assumptions that went into the parameters used for the 50 km environments are discussed in Section 3.1. Following in Section 4, the integral LET spectra, differential fluxes, and integral fluxes generated for the 50 km environments are compared to the DSNE 200 km environments.

3.1   Assumptions

Information about the 3-DOF DAC-1 BOLE separation was provided. The trajectory was optimized to produce maximum loads, so a lower separation altitude is achieved. There also was no dispersion in launch azimuth. The specific data provided is as follows:

3.1.1   BOLE Separation Location

- Altitude (ft): 1.47769768×10^5 to 1.56331111×10^5 (or 45.04 km to 47.65 km)

- Geodetic Latitude (deg): 28.63679 to 28.63769

- Longitude (deg): 279.844269 to 279.892322

- Inclination (deg): 28.48989 to 28.49106

3.1.2   LC-39b Location

In order to include dispersion in launch azimuth, the downrange distance is computed assuming a launch location from KSC launch complex 39b.

- Geodetic Latitude (deg): 28.627623

- Longitude (deg): 279.378890.

3.1.3   Downrange Distance and Initial Bearing

Given the latitude and longitude (ϕ, λ) of the starting and ending location, a downrange distance can be computed[2] using

$$D = 2r_E \arcsin(\sqrt{a}), \tag{5}$$

where $r_E = 6371$ km (Earth's radius), and

$$a = \sin^2(\Delta\phi/2) + \cos\phi_1 \cos\phi_2 \sin^2(\Delta\lambda/2), \tag{6}$$

for $\Delta\phi = \phi_1 - \phi_2$ and $\Delta\lambda = \lambda_1 - \lambda_2$.

---

[2]E.g., see https://www.movable-type.co.uk/scripts/latlong.html

The initial bearing from the launch point can also be calculated using

$$\tan \theta_{i(1,2)} = \frac{\sin \Delta \lambda \cos \phi_2}{\cos \phi_1 \sin \phi_2 - \sin \phi_1 \cos \phi_2 \cos \Delta \lambda}. \tag{7}$$

Therefore, from the initial separation data, the bearing and downrange distance is the following:

- **Nominal bearing** (deg, from N CCW): -88.48 to -88.71 (i.e., almost strictly due East)

- **Downrange distance** (km): 45.4 to 50.1.

The range of valid bearings from KSC LC-39b are $-35°$ to $-120°$, where the worst-case[3] would be $-35°$ (most northerly direction), giving an orbital inclination of $57°$.

3.1.4 Magnetic Epoch and L-Shell

A magnetic epoch must be selected in order to convert geodetic latitude and longitude to magnetic latitude and longitude. The magnetic latitude and separation altitude are used to compute the L-shell. In DSNE, it is implicitly assumed that the magnetic epoch is 1980, driven by the assumptions built into CREME96. However, a magnetic epoch of 2020 is also used in the analysis for the lower bound[4] on the L-shell.

The L-shell can be computed by

$$L = \frac{1 + \frac{h}{R_E}}{\cos(\phi_{\text{geomagnetic}})}, \tag{8}$$

were h is the spacecraft altitude, $R_E = 6371$ km, and $\phi_{\text{geomagnetic}}$ is the geomagnetic latitude.

If a most-northerly(southerly) launch azimuth case is assumed, the magnetic latitude for different magnetic epochs is given in Table 1.

Table 1: The magnetic latitudes at BOLE separation for magnetic epochs of 1980 & 2020 and bounding cases for launch azimuths ($65°$ to $-30°$).

	1980 epoch	2020 epoch
Most-northerly	$39.83°$	$38.14°$
Most-southerly	$39.23°$	$37.54°$

L-Shell Sensitivity: The L-shell sensitivity, or dL, is affected by magnetic epoch, launch azimuth, and separation altitude, summarized below:

---

[3]Worst-case in terms of a larger L-shell value, giving less magnetic field protection from space radiation.
[4]Currently, the magnetic south pole (near the geographic north pole) has been migrating towards the Asian continent, hence putting KSC at a lower L-shell over several decades.

- Magnetic epoch: Magnetic latitude difference of $1.69°$ ($dL \approx 0.08$ or 72% of total dL)

- Launch azimuth: Magnetic latitude difference of $0.60°$ ($dL \approx 0.03$ or 27% of total dL)

- Altitude at separation: Altitude difference of 5 km ($dL \approx 0.0013$ or 1% of total dL)

Therefore, the choice of magnetic epoch drives the range of the L-shell compared to the launch azimuth range and range in separation altitude.

3.1.5 L-Shell Range

Given the analysis in Section 3.1.4, the L-shell range used in deriving the new 50 km environments is:

- From 1.60174 (most southerly launch azimuth, 2020 magnetic epoch, and separation altitude of 45 km)

- To 1.70896 (most northerly launch azimuth, 1980 magnetic epoch, and separation altitude of 50 km).

The difference from using a separation altitude of 47.65 km vs. 50 km changes the L-shell value only in the last two significant figures.

3.2 GTRN, FLUX, and LETSPEC Options for 50 km Environments

The options used in the GTRN routine for the 50 km environments (as a best guess worst-case) are as follows:

- 1.C.a. & 1.C.b. 50 km circular orbit

- 1.C.c. 57 degrees orbit inclination

- 1.C.g. Effective L-shell range: $1.60174 \leqslant L \leqslant 1.70896$

- 2. Stormy magnetic weather conditions.

Options for the FLUX and LETSPEC routines are the same as in Sections 2.2 and 2.1, respectively.

4 Comparison of 50 km and 200 km Environments

4.1 Linear Energy Transfer (LET)
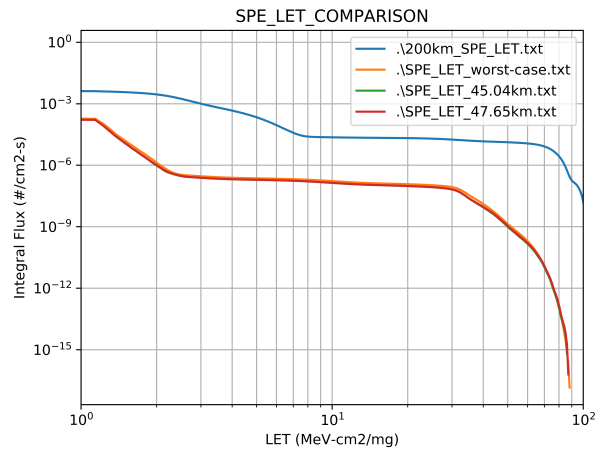
(a) Comparing different SPE LET BOLE environments with 200 km DSNE environment.

(b) Comparing different GCR LET BOLE environments with 200 km DSNE environment.

Figure 4: Comparison of integral LET fluxes between 50 km and 200 km environments.

Table 2: 50 km Integral LET Flux as shown in Figure 4, worst-case lines.

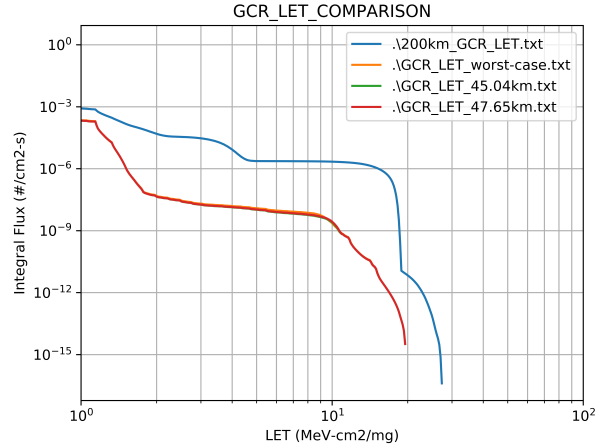| LET (MeV-cm^2/mg)	Design SPE Integral Flux (#/cm^2-s)	GCR Integral Flux (#/cm^2-s)
1.00E+00	1.86E-04	2.23E-04
1.10E+00	1.84E-04	2.04E-04
1.20E+00	1.24E-04	5.81E-05
1.31E+00	5.31E-05	2.04E-05
1.44E+00	2.19E-05	3.32E-06
1.58E+00	1.01E-05	4.63E-07
1.73E+00	4.73E-06	1.21E-07
1.89E+00	2.19E-06	5.80E-08
2.07E+00	9.77E-07	4.33E-08
2.27E+00	4.92E-07	3.53E-08
2.49E+00	3.46E-07	3.04E-08
2.73E+00	3.11E-07	2.44E-08
2.99E+00	2.90E-07	2.03E-08
3.27E+00	2.71E-07	1.82E-08
3.58E+00	2.56E-07	1.71E-08
3.92E+00	2.45E-07	1.58E-08
4.30E+00	2.38E-07	1.47E-08
4.71E+00	2.32E-07	1.33E-08
5.16E+00	2.27E-07	1.16E-08
5.65E+00	2.22E-07	1.00E-08
6.19E+00	2.17E-07	9.19E-09
6.78E+00	2.10E-07	8.47E-09
7.43E+00	2.03E-07	7.90E-09
8.14E+00	1.93E-07	7.17E-09
8.91E+00	1.82E-07	5.79E-09
9.76E+00	1.71E-07	2.92E-09
1.07E+01	1.59E-07	9.12E-10
1.17E+01	1.49E-07	3.93E-10
1.28E+01	1.40E-07	8.18E-11
1.41E+01	1.34E-07	3.83E-11
1.54E+01	1.29E-07	5.54E-12
1.69E+01	1.25E-07	1.04E-12
1.85E+01	1.21E-07	1.10E-13
2.02E+01	1.17E-07	0.00E+00
2.22E+01	1.13E-07	0.00E+00
2.43E+01	1.07E-07	0.00E+00
2.66E+01	1.00E-07	0.00E+00
2.91E+01	9.00E-08	0.00E+00
3.19E+01	6.84E-08	0.00E+00
3.50E+01	3.58E-08	0.00E+00
3.83E+01	1.79E-08	0.00E+00
4.20E+01	8.48E-09	0.00E+00
4.60E+01	3.46E-09	0.00E+00
5.04E+01	1.27E-09	0.00E+00
5.52E+01	5.07E-10	0.00E+00
6.04E+01	1.82E-10	0.00E+00
6.62E+01	4.21E-11	0.00E+00
7.25E+01	4.54E-12	0.00E+00
7.94E+01	1.54E-13	0.00E+00
8.70E+01	2.84E-16	0.00E+00

4.2   Differential Flux
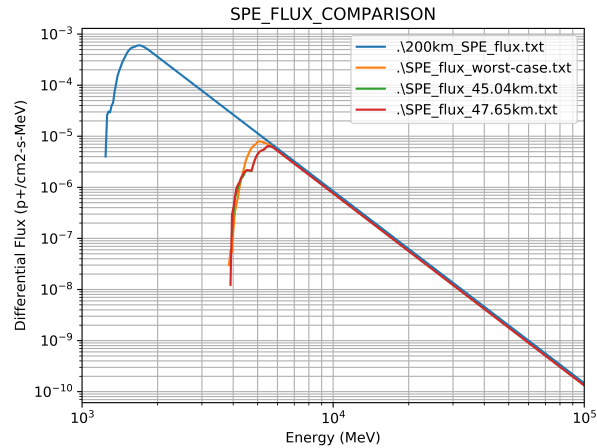
(a) Comparing different differential SPE flux BOLE environments with 200 km DSNE environment.
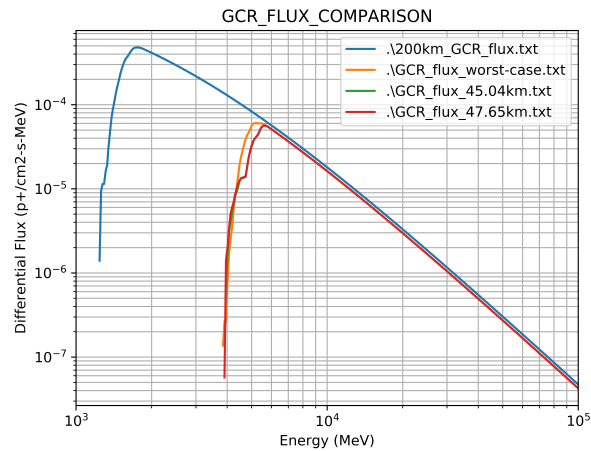
(b) Comparing different differential GCR flux BOLE environments with 200 km DSNE environment.
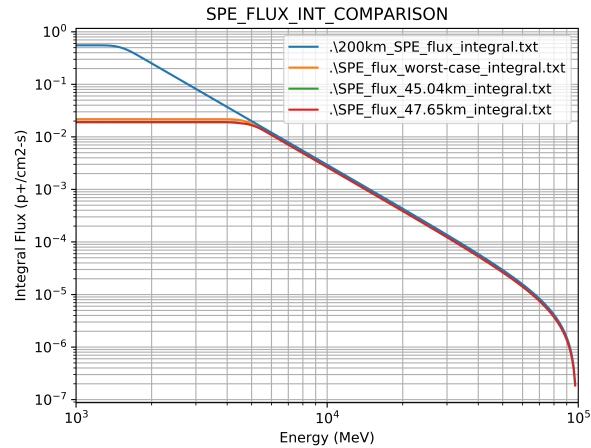
Figure 5: Comparison of differential fluxes between 50 km and 200 km environments.

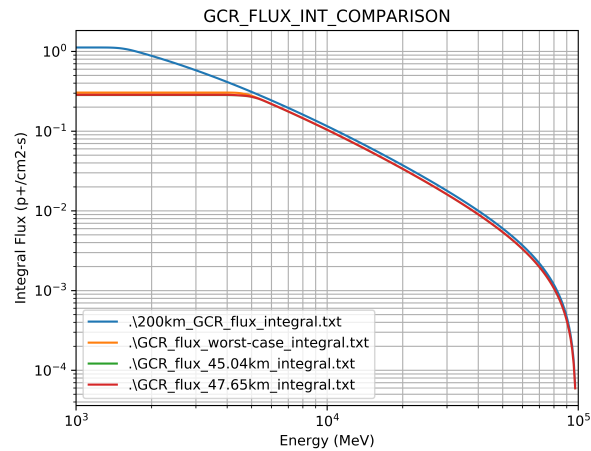Table 3: 50 km Differential Flux as shown in Figure 5, worst-case lines.

Energy (MeV)	Design SPE Differential Flux (p+/cm^2-s-MeV)	GCR Differential Flux (p+/cm^2-s-MeV)
3.90E+03	5.50E-08	2.56E-07
4.17E+03	5.99E-07	3.17E-06
4.45E+03	2.77E-06	1.66E-05
4.75E+03	6.00E-06	4.01E-05
5.08E+03	7.97E-06	5.95E-05
5.42E+03	7.19E-06	6.00E-05
5.79E+03	5.92E-06	5.50E-05
6.19E+03	4.63E-06	4.78E-05
6.61E+03	3.61E-06	4.14E-05
7.06E+03	2.82E-06	3.58E-05
7.55E+03	2.20E-06	3.09E-05
8.06E+03	1.72E-06	2.66E-05
8.61E+03	1.34E-06	2.29E-05
9.20E+03	1.04E-06	1.97E-05
9.83E+03	8.15E-07	1.68E-05
1.05E+04	6.35E-07	1.44E-05
1.12E+04	4.96E-07	1.23E-05
1.20E+04	3.87E-07	1.05E-05
1.28E+04	3.02E-07	8.96E-06
1.37E+04	2.35E-07	7.62E-06
1.46E+04	1.84E-07	6.48E-06
1.56E+04	1.43E-07	5.50E-06
1.67E+04	1.12E-07	4.67E-06
1.78E+04	8.72E-08	3.95E-06
1.90E+04	6.80E-08	3.35E-06
2.03E+04	5.31E-08	2.83E-06
2.17E+04	4.14E-08	2.39E-06
2.32E+04	3.23E-08	2.02E-06
2.48E+04	2.52E-08	1.70E-06
2.64E+04	1.97E-08	1.44E-06
2.82E+04	1.53E-08	1.21E-06
3.02E+04	1.20E-08	1.02E-06
3.22E+04	9.34E-09	8.57E-07
3.44E+04	7.29E-09	7.21E-07
3.68E+04	5.69E-09	6.06E-07
3.93E+04	4.44E-09	5.09E-07
4.20E+04	3.46E-09	4.27E-07
4.48E+04	2.70E-09	3.59E-07
4.79E+04	2.11E-09	3.01E-07
5.12E+04	1.64E-09	2.52E-07
5.47E+04	1.28E-09	2.12E-07
5.84E+04	1.00E-09	1.77E-07
6.24E+04	7.80E-10	1.48E-07
6.66E+04	6.09E-10	1.24E-07
7.12E+04	4.75E-10	1.04E-07
7.60E+04	3.71E-10	8.71E-08
8.12E+04	2.89E-10	7.29E-08
8.68E+04	2.26E-10	6.10E-08
9.27E+04	1.76E-10	5.10E-08
9.90E+04	1.37E-10	4.27E-08

4.3   Integral Flux

(a) Comparing different integral SPE flux BOLE environments with 200 km DSNE environment.

(b) Comparing different integral GCR flux BOLE environments with 200 km DSNE environment.

Figure 6: Comparison of integral fluxes between 50 km and 200 km environments.

Table 4: 50 km Integral Flux as shown in Figure 6, worst-case lines.

	Design SPE	GCR
Energy (MeV)	**Integral Flux (p+/cm^2-s)**	**Integral Flux (p+/cm^2-s)**
3.50E+03	2.17E-02	3.05E-01
3.74E+03	2.17E-02	3.05E-01
4.00E+03	2.16E-02	3.04E-01
4.28E+03	2.14E-02	3.03E-01
4.58E+03	2.04E-02	2.97E-01
4.90E+03	1.84E-02	2.83E-01
5.24E+03	1.57E-02	2.63E-01
5.61E+03	1.31E-02	2.41E-01
6.00E+03	1.09E-02	2.20E-01
6.42E+03	9.04E-03	2.00E-01
6.87E+03	7.50E-03	1.82E-01
7.34E+03	6.23E-03	1.65E-01
7.86E+03	5.17E-03	1.50E-01
8.40E+03	4.29E-03	1.36E-01
8.99E+03	3.56E-03	1.23E-01
9.61E+03	2.96E-03	1.11E-01
1.03E+04	2.46E-03	9.98E-02
1.10E+04	2.04E-03	8.99E-02
1.18E+04	1.69E-03	8.09E-02
1.26E+04	1.40E-03	7.27E-02
1.35E+04	1.16E-03	6.53E-02
1.44E+04	9.66E-04	5.85E-02
1.54E+04	8.01E-04	5.24E-02
1.65E+04	6.64E-04	4.68E-02
1.76E+04	5.51E-04	4.18E-02
1.89E+04	4.56E-04	3.73E-02
2.02E+04	3.78E-04	3.32E-02
2.16E+04	3.13E-04	2.95E-02
2.31E+04	2.59E-04	2.62E-02
2.47E+04	2.14E-04	2.32E-02
2.64E+04	1.77E-04	2.05E-02
2.83E+04	1.46E-04	1.81E-02
3.02E+04	1.21E-04	1.59E-02
3.23E+04	9.93E-05	1.40E-02
3.46E+04	8.17E-05	1.22E-02
3.70E+04	6.70E-05	1.07E-02
3.96E+04	5.48E-05	9.26E-03
4.23E+04	4.47E-05	8.00E-03
4.53E+04	3.63E-05	6.88E-03
4.84E+04	2.93E-05	5.87E-03
5.18E+04	2.35E-05	4.97E-03
5.54E+04	1.87E-05	4.17E-03
5.93E+04	1.47E-05	3.45E-03
6.34E+04	1.14E-05	2.80E-03
6.78E+04	8.67E-06	2.23E-03
7.26E+04	6.39E-06	1.72E-03
7.76E+04	4.49E-06	1.26E-03
8.30E+04	2.91E-06	8.53E-04
8.88E+04	1.60E-06	4.89E-04
9.50E+04	5.14E-07	1.63E-04

5 Results

In general, both the SPE and GCR fluxes[5] were reduced by flying in an altitude of 50 km vs. 200 km, which is to be expected. The peak SPE and GCR fluxes shifted from 1.7×10^3 MeV to 5.1×10^3 MeV (see Figure 5). The shifted peak is due to the lower L-shell the 50 km environment is in. This lower L-shell blocks particles of lower rigidity, and hence filters out the lower energy particles.

The overall integral SPE flux reduced by a factor of $25\mathrm{x}$ whereas the overall integral GCR flux reduced by a factor of $3.7\mathrm{x}$ (see Figure 6). Since the SPE energy spectrum occurs at much lower energies compared to the GCRs, it is expected that more of the SPEs would be shielded by the Earth's magnetic field compared to the GCRs.

At 1 LET (MeV-cm^2/mg), the SPE LET flux reduced by a factor of $22\mathrm{x}$ while the GCR LET flux reduced by a factor of $3.7\mathrm{x}$. However, at 10 LET (MeV-cm^2/mg), the SPE LET flux reduced by a factor of $137\mathrm{x}$ and the GCR LET flux reduced by a factor of $965\mathrm{x}$. Therefore, it is clear to see that the 50 km environments are much more benign compared with the 200 km environments that are in DSNE.

---

[5]Differences in fluxes due to heavy ions were not studied in this analysis.